Frontiers in Bioscience Landmark

*Front. Biosci. (Landmark Ed)* **2022**; 27(9): 270
https://doi.org/10.31083/j.fbl2709270

*Original Research*

# Spatial Transcriptomics Analysis Reveals that CCL17 and CCL22 are Robust Indicators of a Suppressive Immune Environment in Angioimmunoblastic T Cell Lymphoma (AITL)

Jun Du[1,†], Chen Qiu[2,†], Wei-Song Li[3,†], Bing Wang[2], Xin-Le Han[4], Su-Wen Lin[4], Xue-Hang Fu[1], Jian Hou[1,*], Zou-Fang Huang[5,*]

[1]Department of Hematology, Renji Hospital, School of Medicine, Shanghai Jiao Tong University, 200127 Shanghai, China
[2]State Key Laboratory of Experimental Hematology, Institute of Hematology and Blood Disease Hospital, Chinese Academy of Medical Sciences and Peking Union Medical College, 300020 Tianjin, China
[3]Department of Pathology, The First Affiliated Hospital of Gannan Medical University, 341000 Ganzhou, Jiangxi, China
[4]Biomedical Research Institute, Shenzhen Peking University - The Hong Kong University of Science and Technology Medical Center, 518036 Shenzhen, Guangdong, China
[5]Ganzhou Key Laboratory of Hematology, Department of Hematology, The First Affiliated Hospital of Gannan Medical University, 341000 Ganzhou, Jiangxi, China
*Correspondence: nfyyjsjj@126.com (Zou-Fang Huang); houjian@medmail.com.cn (Jian Hou)
[†]These authors contributed equally.
Academic Editor: Graham Pawelec
Submitted: 5 April 2022 Revised: 17 August 2022 Accepted: 18 August 2022 Published: 29 September 2022

**Abstract**

**Background**: T cell lymphoma is a complex and highly aggressive clinicopathological entity with a poor outcome. The angioimmunoblastic T-cell lymphoma (AITL) tumor immune microenvironment is poorly investigated. **Methods**: Here, to the best of our knowledge, spatial transcriptomics was applied for the first time to study AITL. **Results**: Using this method, we observed that AITL was surrounded by cells bearing immune-suppressive markers. CCL17 and CCL22, the dominant ligands for CCR4, were up-regulated, while the expression of natural killer (NK) cell and CD8+ cytotoxic T lymphocyte (CTL) markers decreased. Colocalization of Treg cells with the CD4+ TFH-GC region was also deduced from the bioinformatic analysis. The results obtained with spatial transcriptomics confirm that AITL has a suppressive immune environment. Chemotherapy based on the CHOP regimen (cyclophosphamide, doxorubicin, vincristine plus prednisone) induced complete remission (CR) in this AITL patient. However, the duration of remission (DoR) remains a concern. **Conclusions**: This study demonstrates that AITL has an immune suppressive environment and suggests that anti-CCR4 therapy could be a promising treatment for this lethal disease.

**Keywords:** AITL; spatial transcriptomics; CCL17/CCL22-CCR4 axis; precision medicine

## 1. Introduction

Peripheral T-cell lymphoma (PTCL) consists of approximately 29 highly aggressive disorders with a poor clinical outcome (2017 WHO classification of hematopoietic and lymphoid tissues, Revised 4th edition). T follicular helper (TFH)-derived PTCL (T-FHCL) has special features that distinguish it from other PTCL [1]. The current categories of T-FHCL include three types: angioimmunoblastic T-cell lymphoma (AITL), follicular T-cell lymphoma, and nodal PTCL with a TFH phenotype. Detailed description of the TFH phenotype includes results on a minimum of two and preferably three of the following markers: CD10, BCL6, PD1, CXCL13, CXCR5, and ICOS. The description also includes CD4 and T-cell specific lineage-limited antigens [2].

"Spatial transcriptomics" is a major technical advance that allows visualization and quantitative detection of transcriptome data with spatial resolution. This technique has been developed to investigate adjacent relationships of mRNA in histological tissue sections [3]. It allows the profiling of subpopulations of clinical samples and builds detailed three-dimensional molecular maps via transcriptome information [4,5].

## 2. Methods

Patient material, ethics and consent for publication. The primary untreated lymphoma sample used in this study was collected with written informed consent from the patient and with approval from the relevant human research ethics committee (The First Affiliated Hospital of Gannan Medical University, Ganzhou, Jiangxi, China). Consent included the use of all de-identified patient data for publication. The participant was not compensated.

Tissue handling. The surgeon-excised lymph node tissue was used as the sample for analysis. It was sent for optimal cutting temperature (OCT) embedding and stored at –80 °C.

Histology and immunohistochemical staining. Two independent pathologists (WSL and CQ) evaluated the morphologic features including growth pattern, immune background, tumor size, and cytology. Markers included in the immunohistochemical staining were CD3, CD21, CD30, CD5, CD7, Bcl-6, CD2, CD4, GATA-3, PD-1, CD20, CD10, Bcl-2, C-myc, EBER, PAX-5, CD8, Gram-B, ALK, and TIA-1.

Spatial transcriptomics. Tissue blocks from the OCT procedure were cut into 10-$\mu$m sections and processed using the Visium Spatial Gene Expression Kit (10x Genomics) according to the manufacturer's instructions. Tissue permeabilization was first optimized using the Visium Spatial Tissue Optimization Kit. This was found to be ideal at 18 minutes. Sections were then stained with H&E, imaged using a Leica DM6000 microscope (Wetzlar GmbH, Wetzlar, Germany) under 20$\times$ magnification, and processed for spatial transcriptomics. The resulting complementary DNA library underwent quality control and was then sequenced using an Illumina NovaSeq 6000 system. Cycling conditions were set at 28, 98 and 8 for Read 1, Read 2 and Read 3 (i7 index), respectively.

Visium spatial transcriptomics data processing. Reads were demultiplexed and mapped to the reference genome GRCh38 using Space Ranger software v.1.0.0 (10x Genomics, Pleasanton, California, United States). Count matrices were loaded into Scanpy v.1.8.1 (Neuherberg, Munich, Germany) for all subsequent data filtering, normalization, filtering, dimensional reduction and visualization. After filtering more than 2000 genes and 10000 UMIs, a total of 4697 spots were obtained for downstream analysis.

Spatial deconvolution using Cell2location. Deconvolution of spatial tissue locations was performed using Cell2location v. 0.6a0 (Hinxton, Cambridge, UK). This is a probabilistic model for estimating cell-type proportions for each spot using annotated scRNA-seq data as input. Kleshchevnikov *et al.* [6,7] previously mapped the cell types and cellular compartments in the normal human lymph node. Similarly, we spatially mapped a comprehensive atlas of 34 reference cell types and derived an integrated single-cell transcriptome dataset from human secondary lymphoid organs composed of 73,260 cells to our spatial transcriptomic data. Cell2location was performed using default parameters.

Spatial co-localization of groups of cells. Non-negative matrix factorization (NMF) of cell type abundance estimates from Cell2location was performed to identify the spatial co-occurrence of different cell types. With parameter n_fact equal to 12, this grouped the spatial cell type abundance profiles into 12 factors, representing components that capture co-localized cell types.

Clustering, differential gene expression and gene set enrichment analysis. Clustering was performed using the Leiden clustering algorithm following total count normalization and high variable genes for PCA dimensionality reduction. Clusters were visualized using the UMAP algorithm. Analysis of differential gene expression was performed with the Wilcoxon rank-sum method in Seurat v4.0.3 (New York University, NY, USA) using default parameters. Gene set enrichment analysis (GSEA) was performed using clusterProfiler v4.3.0.991 on the GO and KEGG datasets.

## 3. Results

Herein, we carried out spatial transcriptomics on an AITL patient sample. The flow diagram for this study is shown in Fig. 1. A surgeon excised the involved lymph node and the pathological tissue was sent for optimal cutting temperature (OCT) embedding (Fig. 2a) and tissue optimization. At 18 minutes, an optimal signal was detected with the least RNA diffusion and the most explicit organizational structure (Fig. 2b). The RNA integrity number (RIN) test score was 8.7, which qualified for the follow-up experiment. The n-Count of UMI and n-Feature of genes per spot were used for quality control (2000 and 4658, respectively; Fig. 2c,d). The spatial analysis of normal lymph nodes as revealed in previous studies [6,7] is shown in Fig. 2e.

The AITL patient in this study was a 68 year-old female admitted to hospital due to swollen lymph nodes in the left neck. Multiple enlarged lymph nodes were found in the left neck, left clavicle fossa, left axillary, mediastinum and right hilum, abdominal cavity, retroperitoneum, and the left iliac vascular area. A diagnosis of lymphoma derived from TFH cells (AITL) was made by two independent pathologists. Destruction of normal lymphatic follicular structure could be observed, as well as hyperplasia of endothelial venules. Immunohistochemistry showed positive staining for CD3, CD21, CD30, CD5, CD7, Bcl-6, CD2, CD4, GATA-3, and PD-1, and negative staining for CD20, CD10, Bcl-2, C-myc, EBER, PAX-5, CD8, Gram-B, ALK, and TIA-1 (Fig. 1). These characteristics concur precisely with the definition of AITL origin. Results shown in **Supplementary Fig. 1** also confirmed the TFH origin of the sample. The patient was therefore diagnosed as AITL stage IV without systematic B symptoms (fever above 38 °C, drenching night sweats, and weight loss >10% of body mass in the previous 6 months).

As deduced from recent pathophysiological studies [1,8,9], the circled part of the CD4+ TFH-GC region shown in Fig. 2f was considered the origin of tumor cells. We conducted differentially expressed gene (DEG) analysis of the CD4+ TFH-GC region versus normal counterpart. A $Log_2$ fold-change ($|log_2FC|$) of >1 and an adjusted $p$-value of <0.05 were set as the filter criteria for DEGs. Amongst the up-regulated genes, chemokine (C-C motif) ligand 17 (CCL17) and CCL22 were the most noteworthy (Fig. 2g). Importantly, adjacency relation analysis of the patient lymph node revealed that Tregs were close to CD4+ TFH (Fig. 2h,i). The circled area originated from the patient, while Fig. 2i shows the normal control. Spa-

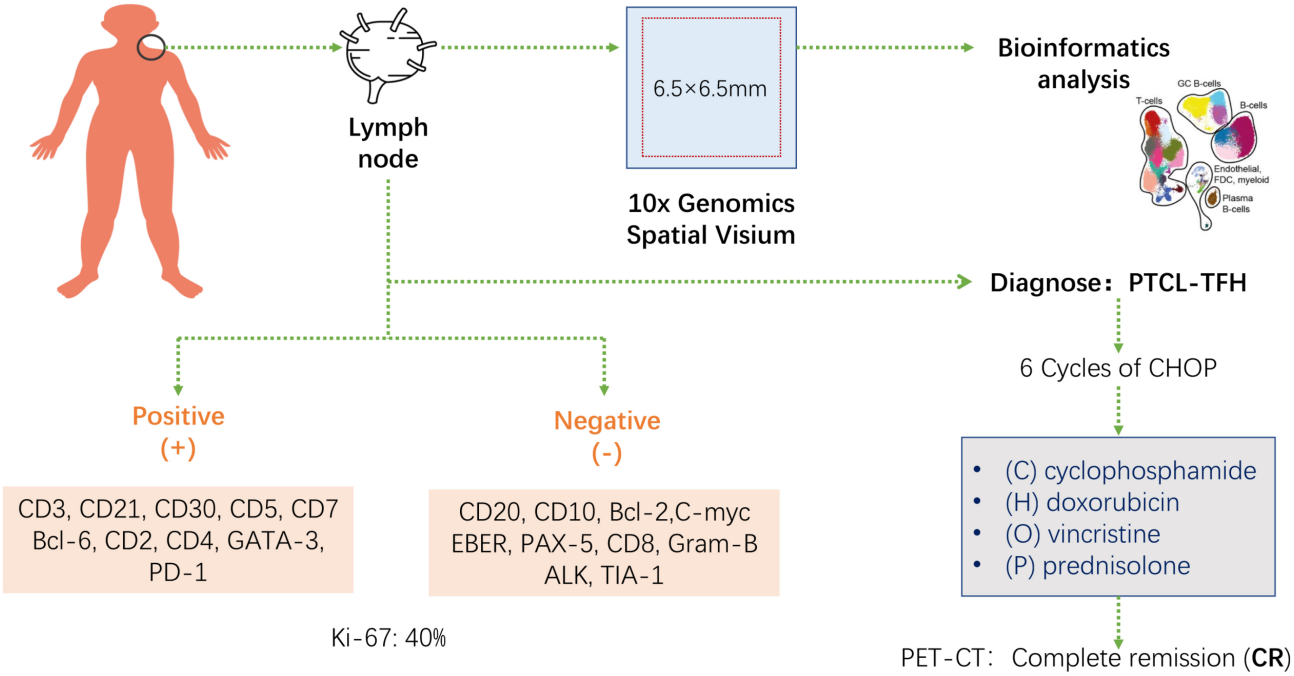


**Fig. 1. Flow diagram of this study and clinical outcome of the AITL patient.** The flow diagram depicts the study program. The diagnosis of AITL was reached based upon morphological features and immunohistochemistry. Evaluation by PET-CT showed CR after six cycles of CHOP chemotherapy.

tial co-localization analysis [10] also implied the interesting phenomenon of CD4+ TFH-GC being nearby to Treg cells (Fig. 2j,k).

Additionally, spatial transcriptomics confirmed an increased level of B cycling cells and of vascular smooth muscle cells (VSMC), but a decreased level of NK cells and CD8+ cytotoxic T lymphocytes (CTL) in the core lesion area (**Supplementary Fig. 2**). These features were all indicative of a suppressive immune environment. A scattered distribution of immune defense cells and up-regulation of Treg-associated markers commonly indicate that malignant T cells were in the stage of immune escape.

The patient received six cycles of CHOP regimen as induction therapy, comprised of cyclophosphamide, doxorubicin, vincristine, and prednisone. Positron emission tomography-computed tomography (PET-CT) and bone marrow aspiration were used to evaluate the efficacy, with complete remission (CR) being demonstrated. Regular follow-up is still ongoing as of July 2022, with chidamide given as maintenance therapy.

## 4. Discussion

CCL17 and CCL22 are known to be the dominant ligands for CCR4, which is expressed diffusely on malignant T cells and Tregs [11]. The interaction between CCR4 and CLL17/CCL22 plays a vital role in the context of cutaneous T-cell lymphoma (CTCL) by recruiting CCR4-expressing Treg cells into the tumor microenvironment. A previous study demonstrated up-regulation of CCR4 in advanced mycosis fungoides (MF) and Sezary syndrome (SS), with both of these diseases originating from malignant T cells [11]. In the phase III MAVORIC (KW-0761) trial, relapsed PTCL and CTCL patients treated with the anti-CCR4 monoclonal antibody mogamulizumab experienced prolonged overall survival (OS) and progression-free survival (PFS). Mogamulizumab (1.0 mg/kg) was administered intravenously once per week for 8 weeks. Objective responses were observed in 13 of 37 patients (35%; 95% CI, 20% to 53%), including 5 patients (14%) with CR [12]. Hence, the novel agent mogamulizumab currently provides a practical option for CTCL patients [13,14].

Our spatial analysis of this AITL patient revealed a suppressive immune environment in which Treg cells were transcriptionally co-expressed with CD4+ TFH-GC. Moreover, the expression of both CCL17 and CCL22 was markedly up-regulated. Since these ligands are the dominant chemokines for the CCR4 axis, our results suggest that targeting CCR4 through down-regulation of Treg cell recruitment could be used to treat AITL [15,16].

PTCL is a heterogeneous and aggressive disease with a dismal prognostic outcome. Recently, it was hypothesized that neoplastic TFH cells play a role in the initiation and development of AITL, follicular T-cell lymphoma and nodal PTCL with the TFH phenotype [17,18]. The application of spatial transcriptomics in the present study of lymphoma found that the three-dimensional tumor environment of AITL was immune-suppressive. Importantly, the expression of CCR4 and of its ligands CCL17 and CCL22 were

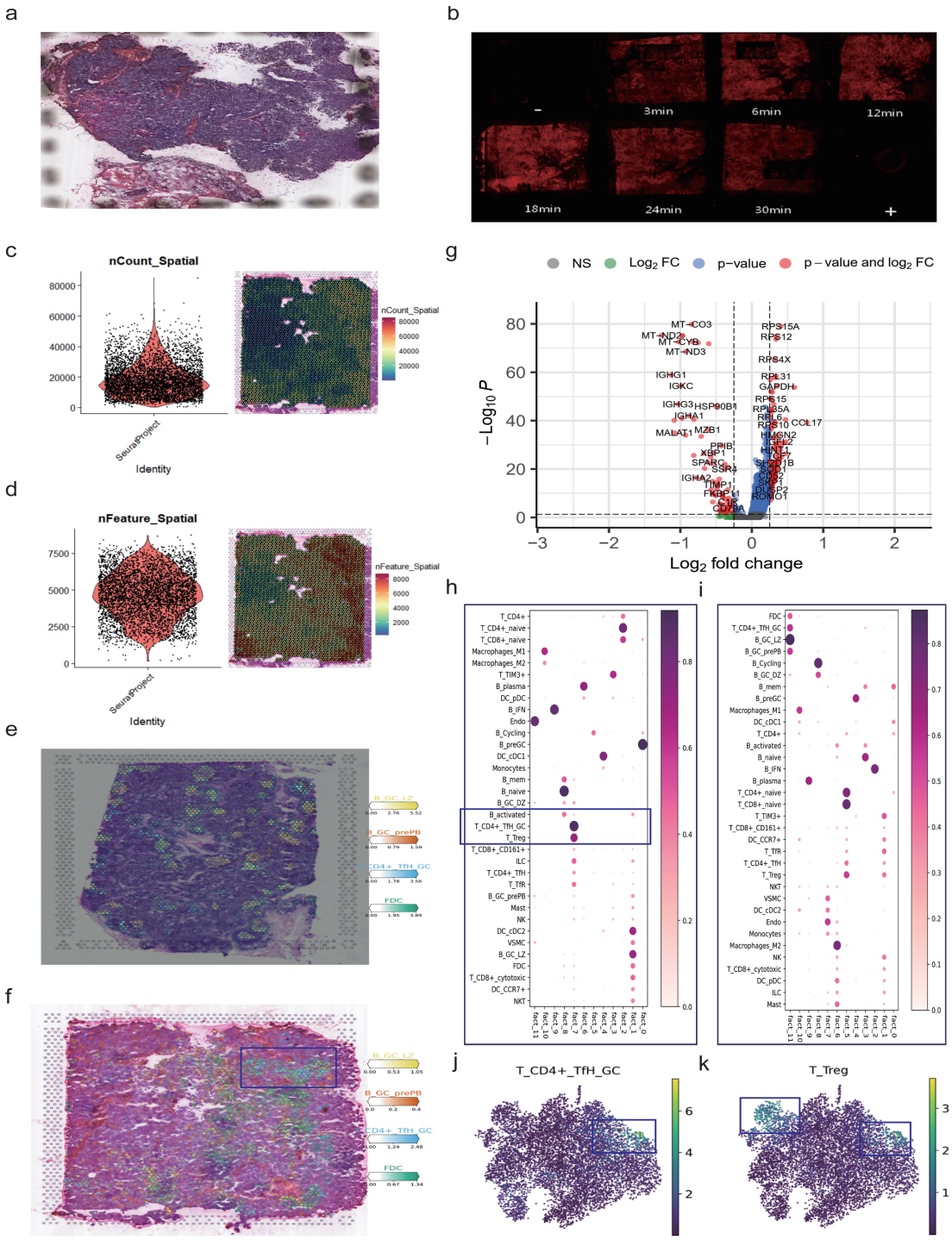


**Fig. 2. Spatial transcriptome results obtained with the AITL clinical sample.** (a) Brightfield microscope scan of the involved lymph node located on the left side of the neck. (b) Tissue optimization of mRNA. A time of 18 minutes gave the strongest fluorescence signal, minimum diffusion of mRNA, and clearest internal organizational structure. (c,d) Quality control of cDNA expression: (c) n-Count of UMI (unique molecular identifier), with a median n-Count of 2000. (d) n-Feature of genes per spot, with a median of 4658 genes after filtering. (e) normal lymph node control from a public database, showing regular immune cell distribution around the germinal center (GC). (f) involved lymph node from the AITL patient. The circled part is the CD4+ TFH-GC region. (g) Differentially expressed gene (DEG) analysis of the region in which Tregs and TFH-GC were co-located. Up-regulated DEGs included CCL17 and CCL22, both of which are core chemokine factors for Tregs. (h,i) Spatial adjacency relations for lymphocyte subsets. (h) Adjacency relation analysis of the AITL patient lymph node revealed that Tregs were close to CD4+TFH. (i) Normal human lymph node control from the public database. (j,k) Co-location of CD4+TFH-GC and Tregs is shown in the circled area, demonstrating spatial co-expression of these cell types.

significantly up-regulated, thus supporting the clinical development of CCR4 inhibitors for use in combination with conventional chemotherapy.

The presence of Treg cells and the CCL17/CCL22-CCR4 axis in the tumor immune microenvironment has been widely investigated in various cancer types. However, the application of spatial transcriptomics in this field is a novel and challenging technique. The precise diagnosis of AITL remains a challenge for clinical pathologists, while the molecular origin of this life-threatening disorder also requires further investigation. The current study using spatial transcriptomics may provide a novel paradigm for lymphoma research. Molecular network regulation involving the CCL17/CCL22-CCR4 axis is a promising area for further clinical translational research and might identify new therapeutic targets, especially in the relapsed and refractory settings. Moreover, bioinformatic analysis of the CCL17/CCL22-CCR4 axis and its interaction with Treg cells should provide further biological validation of this paradigm.

## 5. Conclusions

In summary, the use of spatial transcriptomics in this study revealed up-regulation of CCL17 and CCL22 and a suppressive immune environment in AITL. These results suggest that CCR4 antagonist could therefore be an option for clinical use against this disease. Although a larger sample size is needed for confirmation, this work suggests a pathway towards the precision treatment of AITL.

## Data Availability

All raw data was stored in a database in the School of Medicine, Shanghai Jiaotong University. Anyone wishing to reanalyze the original material or to collaborate with us may contact the corresponding authors. We are pleased to share the bioinformatic analysis of the spatial transcriptome. Furthermore, clinical pathologists specializing in this area are welcome to collaborate with us for the aim of constructing a three-dimensional atlas of the immune microenvironment in PTCL.

## Author Contributions

JH and ZH contributed to the design and guided the promotion of the whole work. JD, CQ and WL carried out this study. SL, XH, BW, and XF anticipated in the data collection and analysis. JD and CQ wrote the manuscript and approved the final submission of the study. All authors were involved in reviewing and revising the manuscript and approved the final manuscript.

## Ethics Approval and Consent to Participate

The primary untreated lymphoma sample used in this study was collected with written informed consent from the patient and with approval from the relevant human research ethics committee (The First Affiliated Hospital of Gannan Medical University, Jiangxi, China) (No. LLSL2022082501). Consent included the use of all deidentified patient data for publication. The participant was not compensated.


## Acknowledgment

Not applicable.

## Funding

This study was funded by the Youth Start-Up Fund for The First Affiliated Hospital of Gannan Medical University (QD081).


## Conflict of Interest

The authors declare no conflict of interest.

## Supplementary Material

Supplementary material associated with this article can be found, in the online version, at https://doi.org/10.31083/j.fbl2709270.

## References


[1] Swerdlow S, Campo E, Harris NL, Jaffe ES, Pileri SA, Stein H, *et al*. WHO classification of tumours of haematopoietic and lymphoid tissues (Revised 4th edition) (pp. 421). IARC: Lyon. 2017.

[2] Zhang X, Zhou J, Han X, Wang E, Zhang L. Update on the Classification and Diagnostic Approaches of Mature T-Cell Lymphomas. Archives of Pathology & Laboratory Medicine. 2021; 146: 947–952.

[3] Ståhl PL, Salmén F, Vickovic S, Lundmark A, Navarro JF, Magnusson J, *et al*. Visualization and analysis of gene expression in tissue sections by spatial transcriptomics. Science. 2016; 353: 78–82.

[4] Burgess DJ. Spatial transcriptomics coming of age. Nature Reviews Genetics. 2019; 20: 317–317.

[5] Baccin C, Al-Sabah J, Velten L, Helbling PM, Grünschläger F, Hernández-Malmierca P, *et al*. Combined single-cell and spatial transcriptomics reveal the molecular, cellular and spatial bone marrow niche organization. Nature Cell Biology. 2020; 22: 38–48.

[6] James KR, Gomes T, Elmentaite R, Kumar N, Gulliver EL, King HW, *et al*. Distinct microbial and immune niches of the human colon. Nature Immunology. 2020; 21: 343–353.

[7] Park JE, Botting RA, Domínguez Conde C, Popescu DM, Lavaert M, Kunz DJ, *et al*. A cell atlas of human thymic development defines T cell repertoire formation. Science. 2020; 367: eaay3224.

[8] Timmins MA, Wagner SD, Ahearne MJ. The new biology of PTCL-NOS and AITL: current status and future clinical impact. British Journal of Haematology. 2020; 189: 54–66.

[9] Fiore D, Cappelli LV, Broccoli A, Zinzani PL, Chan WC, Inghirami G. Peripheral T cell lymphomas: from the bench to the clinic. Nature Reviews Cancer. 2020; 20: 323–342.

[10] Fawkner-Corbett D, Antanaviciute A, Parikh K, Jagielowicz M, Gerós AS, Gupta T, *et al*. Spatiotemporal analysis of human intestinal development at single-cell resolution. Cell. 2021; 184: 810–826.e23.

[11] Nicolay JP, Albrecht JD, Alberti-Violetti S, Berti E. CCR4 in cu-

taneous T-cell lymphoma: Therapeutic targeting of a pathogenic driver. European Journal of Immunology. 2021; 51: 1660–1671.
[12] Ogura M, Ishida T, Hatake K, Taniwaki M, Ando K, Tobinai K, *et al*. Multicenter Phase II Study of Mogamulizumab (KW-0761), a Defucosylated Anti-CC Chemokine Receptor 4 Antibody, in Patients with Relapsed Peripheral T-Cell Lymphoma and Cutaneous T-Cell Lymphoma. Journal of Clinical Oncology. 2014; 32: 1157–1163.
[13] Mogamulizumab Tops Standard of Care for CTCL. Cancer Discovery. 2018; 8: OF1.
[14] Kempf W, Mitteldorf C. Cutaneous T-cell lymphomas—an update 2021. Hematological Oncology. 2021; 39: 46–51.
[15] Marshall LA, Marubayashi S, Jorapur A, Jacobson S, Zibinsky M, Robles O, *et al*. Tumors establish resistance to immunotherapy by regulating T(reg) recruitment via CCR4. Journal for Immunotherapy of Cancer. 2020; 8: e000764.
[16] Sato T, Coler-Reilly ALG, Yagishita N, Araya N, Inoue E, Furuta R, *et al*. Mogamulizumab (Anti-CCR4) in HTLV-1–Associated Myelopathy. New England Journal of Medicine. 2018; 378: 529–538.
[17] Chiba S, Sakata-Yanagimoto M. Advances in understanding of angioimmunoblastic T-cell lymphoma. Leukemia. 2020; 34: 2592–2606.
[18] Marchi E, O'Connor OA. The rapidly changing landscape in mature T-cell lymphoma (MTCL) biology and management. CA: A Cancer Journal for Clinicians. 2020; 70: 47–70.